Available online at www.sciencedirect.com
ScienceDirect
Polymer 48 (2007) 4503–4510
polymer
www.elsevier.com/locate/polymer

Structure of poly(vinyl pyrrolidone) − C_{70} complexes in aqueous solutions

Elvira Tarassova [a], Vladimir Aseyev [b,*], Alexander Filippov [a], Heikki Tenhu [b]

[a] *Institute of Macromolecular Compounds, Russian Academy of Sciences, Bolshoi Prospect 31, 199004 St. Petersburg, Russia*
[b] *Laboratory of Polymer Chemistry, PB 55, FIN-00014 HY, University of Helsinki, Finland*

Received 13 February 2007; received in revised form 16 May 2007; accepted 17 May 2007
Available online 2 June 2007

Abstract

Aqueous solutions of poly(vinyl pyrrolidone)−fullerene complexes, PVP/C_{70}, have been studied using static and dynamic light scattering. Two diffusive processes were observed. The slow diffusion describes the motion of large PVP/C_{70} clusters, whereas the fast diffusion is associated with the presence of single PVP molecules or small individual PVP/C_{70} complexes of the order of a single PVP chain. The molar mass and the size of the PVP/C_{70} clusters increase upon increasing the fullerene content. However, when the fullerene content is kept constant, an increase in the molar mass of the matrix PVP does not influence the mass and the size of the clusters. Dilution of the PVP/C_{70} solutions has no effect on the clusters either. In PVP/C_{70} there is a specific molar ratio of C_{70} per repeating units of PVP that is same for all the samples studied.

Keywords: Polymer−fullerene complex; Aqueous solutions; Light scattering

1. Introduction

Due to their unique shape and distribution of the π-electrons, fullerenes have recently found their application in various areas of engineering, chemistry, medicine and biology [1,2]. However, the hydrophobicity of fullerenes limits their application. Intermolecular complexes formed between fullerenes and water-soluble polymers provide a solution for this problem. As has recently been revealed, the complexes of poly(*N*-vinyl pyrrolidone), PVP, with fullerene C_{60} are formed via the donor−acceptor mechanism of binding between the fullerene and the carbonyl groups of the polymer [3–5]. Such a complex consisting of one PVP molecule and fullerene is named as an individual complex. In the fullerene containing complexes the initial structure of fullerene is almost intact [5]. PVP/C_{60} complex exhibits an antiviral activity and may be used in medicine [6].

Properties of aqueous solutions of the PVP/C_{60} complexes have been investigated by means of NMR, UV, static, SLS, and dynamic, DLS, light scattering, sedimentation−diffusion analysis and viscometry [2–9]. As has been shown, the hydrophobic association of the fullerenes competes with the hydrophilic repulsion between the polymer molecules and results in strong intermolecular interactions [7–9]. Aqueous solutions of pure PVP as a matrix polymer and its complexes with fullerene C_{70} were also studied [10,11]. However, the structure and dynamics of the PVP−fullerene complexes based on the fullerene C_{70} have not been enough investigated.

Static light scattering experiments on aqueous solutions of PVP/C_{70} and PVP/C_{60} demonstrated that the reciprocal reduced intensity of scattered light, $cK/I_{\theta=90^\circ}$, does not exhibit a usual linear dependence in the range of polymer concentrations, where the solutions are expected to be dilute. Thus, above a certain critical concentration of the PVP−fullerene solution, $c_c \approx 1.8$–2.3 mg/ml, the scattering intensity, I_θ, is independent of concentration at least until the highest measured concentration of 4–5 mg/ml, i.e. $cK/I_{\theta=90^\circ} = \text{const} \times c$ and the measuring of a true molar mass is not possible. On the

* Corresponding author. Tel.: +358 9 19150335; fax: +358 9 19150330.
E-mail address: vladimir.aseyev@helsinki.fi (V. Aseyev).

0032-3861/$ - see front matter © 2007 Elsevier Ltd. All rights reserved.
doi:10.1016/j.polymer.2007.05.069

other hand, when $c < c_c$, the extrapolation to zero concentration provides well defined values of the molar mass. Values of M_w^{app} obtained for the PVP/fullerene complexes were 1–2 orders of magnitude higher than those for the pure matrix PVP. It has been suggested that the multi-molecular associates, *clusters*, exist in dilute solutions of PVP/fullerene complexes below c_c and that the clusters form a loose transient network above c_c. This implies that for the PVP/fullerene complexes the crossover concentration, c^*, is actually as low as $c_c \approx$ 1.8–2.3 mg/ml, which is significantly lower than one can expect for single PVP molecules of the molar mass studied ($c^* \sim 50$ mg/ml and higher).

In our earlier publications [7–11] the SLS and DLS experiments on PVP/C_{70} complexes have been mainly performed at 90° scattering angle, although the solutions dissymmetry of the scattered light, $z_\theta = I_\theta / I_{180^\circ-\theta}$, has been studied as well. Taking into account the existing angular dependence of the scattered light intensity, one may expect that the actual molar masses obtained at 0° are even higher than the apparent values obtained at 90°. Moreover, the presence of the fast diffusive process in PVP/C_{70} solution perturbs the obtained values of molar masses and sizes of the clusters. Indeed, the molar mass obtained using SLS is a weight-average value and thus equals $M_{w,f}w_f + M_{w,s}w_s$, where the subscripts "f" and "s" denote to the lower (fast diffusion) and higher (slow diffusion) molar mass scatterers, respectively; $w_f = c_f/c$ and $w_s = c_s/c$ are the relative weight fractions, and $w_f + w_s = 1$. As a result, the crossover concentration c^* of clusters is misleading if estimated using the measured average M_w. The internal organization of the polymer/fullerene clusters and the difference in associating properties of C_{60} and C_{70} have not been elucidated in our previous research [10,11].

Therefore, the main aim of the present study is to find out the actual molecular parameters, mass, size, shape and the internal organization of the PVP/fullerene C_{70} clusters in aqueous solutions using simultaneous static and dynamic light scattering measurements. To estimate the cluster parameters, the relative contributions from the two observed scattering species (fast and slow diffusion) to the total intensity of scattered light should be evaluated and analyzed separately. These contributions can be obtained from the DLS data, in particular from the intensity weighted distributions of the hydrodynamic radius. Since the solutions of the PVP/C_{70} complexes have already been proven to consist of two well-defined scattering species, these PVP/fullerene complexes were chosen for the detailed quantitative analysis.

2. Experimental

2.1. Materials

The PVP–fullerene complexes were prepared from poly(vinyl pyrrolidone), PVP, of $M_w = 10 \times 10^3$, 25×10^3, 40×10^3, 46×10^3 g/mol with $M_w/M_n \cong 1.1$–1.3 (Merck) and the fullerene C_{70} of 98% purity (*Fullerene Technologies*, Russia) using the method described in Ref. [12]. In this method benzene solutions of pure polymer and fullerene are mixed together, and the solvent is evaporated. All polymer samples were characterized by static light scattering in aqueous solutions before the mixing. The PVP/C_{70} complexes were prepared with various relative C_{70} content, ϕ, ranging from 0.28 to 0.63 wt% with respect to the mass of pure PVP in the mixture. Fullerene content in the complexes was determined from the UV absorption spectra of the aqueous solutions of the samples. Table 1 represents the compositions and the molecular parameters of the investigated samples.

Aqueous solutions were prepared from dry PVP/C_{70} in deionized water. Water was purified and deionized with an ELGASTAT UHQ-PS device. The solutions were purified of dust using filter units of 0.45 μm pore size (Millex, PVDF filter). To verify that the concentration of solutions does not change after filtration we conducted the following procedure. We weighed the filter before and after filtration of solution (filter was dried from solvent). As expected, the mass loss amounts only about 1–2% from initial value as a consequence of filtering.

2.2. Instrumentation

Light scattering experiments were performed using a Brookhaven Instrument BIC-200 SM goniometer and BIC-9000 AT digital correlator. An argon laser (LEXEL 85, 1 W) operating with $\lambda = 514.5$ nm wavelength was the light source. Correlation functions were collected with the shortest sample time

Table 1
Static and dynamic light scattering results for aqueous solutions of PVP/C_{70} complex obtained at 0° scattering angle

No.	Matrix polymer		ϕ, wt%	Data before deconvolution			Fast mode (weighted data)		Slow mode (weighted data)		
	$M_{PVP} \times 10^{-3}$, g/mol	R_h, nm		$M_{w,tot} \times 10^{-5}$, g/mol	R_g, nm	R_h, nm	$M_{w,f} \times 10^{-3}$, g/mol	$R_{h,f}$, nm	$M_{w,s} \times 10^{-6}$, g/mol	$R_{g,s}$, nm	$R_{h,s}$, nm
1	10		0.28	2.8	86	65	15	2.3	4.2	94	53
2	10	3.0	0.40	6.8	107	104	8	2.2	4.9	103	73
3	10		0.63	51	215	150	11	3.8	62	242	130
4	25		0.40	2.5	98	97	21	5.6	4.8	106	74
5	25	5.2	0.62	110	254	136	24.5	5.6	71	250	114
							20*	4.5*	75*	260*	110*
6	40	7.0	0.40	6.0	94	98	34	6.4	5.1	96	71
7	40		0.63	97	162	134	40	6.0	70	230	127
8	46		0.55	85	242	130	40	6.0	75	260	118

* Data obtained using the modified method that takes into account the shape of the distributions of relaxation times, see Eq. (12).

0.1–2.0 μs, whereas the last delay was 8–10 ms. Data was analyzed with Brookhaven Instruments software (6KDLSW, Beta version 1.30). The BIC device was calibrated using toluene. Scattered light was collected between 45° and 150° scattering angles in both static and dynamic light scattering experiments. Five to seven correlation curves with various accumulation times were collected for every sample to get proper average values and to verify the mathematical solution obtained with an inverse Laplace transform program CONTIN. The average error of the CONTIN residuals was less than 5×10^{-2}. The difference between the calculated and measured baselines of the correlation functions collected was less than 0.5%. Refractive index increment dn/dc was measured with an IRF 23 refractometer. The dn/dc values for solutions of PVP/C_{70} complexes with varying fullerene content were $dn/dc = 0.171 \pm 0.002$ ml/g. For pure PVP dn/dc was 0.167 ± 0.002 ml/g. The experiments were performed at 20 °C ± 0.1 °C.

2.3. Methods

In static light scattering experiments, the time-averaged intensity of scattered light was collected as a function of sample concentration c and scattering angle θ. When extrapolated to zero scattering angle and zero concentration, such measurements yield the weight-averaged molar mass, $M_{w,}$ the radius of gyration, R_g, and the second osmotic virial coefficient, A_2, of the scattering objects [13].

$$\frac{cK}{I_\theta} = \frac{1}{P(\theta)M_w} + 2A_2c \tag{1}$$

where K is the optical constant given by

$$K = \frac{4\pi^2 n_0^2 (dn/dc)^2}{N_A \lambda_0^4} \tag{2}$$

In Eqs. (1) and (2), I_θ is the excess intensity of light scattered at the angle θ represented as the Rayleigh ratio; cK/I_θ is the reciprocal of reduced scattering intensity; $P(\theta)$ is the particle scattering factor representing angular dependence of scattered light; N_A is the Avogadro number; λ_0 is the wavelength of the incident laser light source; n_0 is the refractive index of the solvent.

In dynamic light scattering experiments, the autocorrelation function of scattered light intensity $G_2(t) = \langle I(0)I(t)\rangle$ was collected and then converted into an autocorrelation function of the scattered electric field $g_1(t)$ using the Siegert's relationship [14]

$$|g_1(t)| = \beta^{1/2}\left\{\left(\frac{G_2(t) - G_2(\infty)}{G_2(\infty)}\right)^{1/2}\right\} \tag{3}$$

where $G_2(\infty)$ is the experimentally determined baseline, β is the coherence factor determined by the geometry of the detection. Time correlation functions were analyzed with program CONTIN by fitting correlation curves as

$$g_1(t) = \int_0^\infty A(\tau)e^{-1/\tau}\, d\tau \tag{4}$$

where $A(\tau)$ is a distribution function of decay times.

Translation diffusion coefficients were calculated as $D = (1/\tau)q^{-2}$, where q is the scattering vector determined as $q = 4\pi n_0/\lambda_0 \sin\theta/2$. The hydrodynamic radius was obtained from the diffusion coefficient D via the Stokes–Einstein equation

$$R_h = \frac{kT}{6\pi\eta_0 D} \tag{5}$$

where k is the Boltzmann constant, T is the absolute temperature, and η_0 is the solvent viscosity. Mean average values of the hydrodynamic radius distributions were used for the estimation of the average radius, R_h.

PVP/C_{70} samples were investigated using static, SLS, and dynamic, DLS, light scattering for 10 scattering angles, q, ranging from 45° to 150° and 4–6 solution concentrations in the range of concentration below the critical concentration c_c. The autocorrelation functions of scattered light intensity $G_2(q,t) = \langle I(q,t=0)I(q,t)\rangle$ were recorded simultaneously with the integral scattering intensities $I(q)$ (the total absolute excess intensities of scattered light). The angular and concentration dependences of intensity, $I(q)$, and the distributions of the hydrodynamic radius, R_h, were analyzed.

3. Results and discussion

To avoid problems with semi-dilute solutions, dilute PVP/C_{70} complexes were investigated below the critical concentration of $c_c = c^* = 2.3$ mg/ml. As has previously been suggested [11], an external hydrodynamic field can easily destroy the clusters and viscosity of PVP/C_{70} may coincide with that of the pure matrix PVP. Thus the overlap concentration c^* estimated using the intrinsic viscosity of the PVP/C_{70} complexes $c^* = 1/[\eta]$ (shear stress of 100–1000 s^{-1}) is in the range of 50–100 mg/ml, which is 1 order of magnitude higher than the critical concentration c_c. Therefore, PVP/C_{70} solutions are certainly expected to be dilute below c_c. According to the static light scattering results, when $c < c_c$ the power ξ in $I_\theta \sim c^\xi$ equals 1 for the PVP/C_{70} solutions and the application of the classical light scattering theory is valid for calculation of the molar mass and size of the clusters.

Two well-separated peaks in the distribution of the relaxation times of the correlation functions have been detected for all the samples studied at all the scattering angles. For each peak the mean peak values of τ_f and τ_s were calculated. Dependence of the decay rate of correlation functions $\Gamma = 1/\tau = Dq^2$ vs. scattering vector q^2 for either of the peaks is linear and passes through the center of coordinates thus representing a true diffusive process. Consequently, two dynamic modes can be analyzed individually and the corresponding diffusion coefficients and the relative amplitudes can be calculated.

Each scattering species of the radius $R_{h,i}$ is represented in the intensity weighted size distribution by its relative contribution, i.e. by the amplitude $A_i(\tau_i)$, to the total intensity of the scattered light. The relative amplitudes of the slow and fast relaxation processes have been estimated using the procedure outlined in works [15,16] as

$$A_f \equiv \sum_{fast} A_i(\tau_i) \text{ and } A_s = 1 - A_f \quad (6)$$

Then we converted the relative amplitudes of the diffusive modes into the intensities of the light scattered by the particles of each type. The time-average intensities $I_f(q)$ and $I_s(q)$ associated with the concentration fluctuations with respect to the short and long relaxation processes were obtained as

$$I_f(q) = A_f(q)I(q) \text{ and } I_s(q) = A_s(q)I(q)[0,1] \quad (7)$$

As is well known, the large particles (clusters) scatter more light than the small particles (PVP). Even small quantities of the large particles may dominate the overall scattering. Therefore, amplitudes A_i of the size distribution can be weighted further to obtain a mass weighted size distribution. The mass weighted distribution is calculated directly from the intensity distribution via Rayleigh equation. Thus, the scattering intensity of ith particle, I_i, is proportional to the molar mass, M_i, and the mass concentration, c_i, of the particle

$$I_i \sim M_i c_i \quad (8)$$

In its turn, $M_i \sim R_i^x$, where R_i is the size of the ith particle, x is a shape parameter that equals 2 for ideal coils and 3 for spheres. Eq. (8) can be rewritten as

$$I_i \sim R_i^x c_i \text{ or } c_i \sim I_i/R_i^x \quad (9)$$

Knowing the total concentration c of the PVP/C_{70} solution, the concentration of the individual molecules, c_f, and clusters, c_s, in solutions can be estimated, assuming coil-like conformation of both scattering species. The relative weight content of the ith particle is then defined as

$$w_i = \frac{I_i/R_i^x}{\sum I_i/R_i^x} \quad (10)$$

In our previous work [10] we have already estimated the R_g/R_h ratio for one of the PVP/C_{70} complexes that had relatively high C_{70} content. That sample showed no fast mode within the whole range of the scattering angles studied. R_g/R_h ratio was 1.7, which is typical for moderately polydisperse ideal coils [17]. Besides, the experimental scattering function $P(q) = I_s(q)/I_s$ $(q = 0)$ was typical for a coil-like structure. Taking that into account, we applied the coil model to the PVP/C_{70} clusters (as well as for the PVP molecules) and input $x = 2$ to Eq. (10) to estimate the concentrations of scattering species

$$w_f = \frac{c_f}{c} = \frac{\sum_{fast} \frac{A_i}{R_{h,i}^2}}{\sum_{fast} \frac{A_i}{R_{h,i}^2} + \sum_{slow} \frac{A_i}{R_{s,i}^2}} \text{ and } w_s = \frac{c_s}{c} = 1 - w_f \quad (11)$$

The example of such conversion from the original intensity weighted size distribution to the mass weighted size distribution is shown in Fig. 1 for the sample 3.

From the mass weighted size distribution (Fig. 1b) the mean values of the apparent $R_{h,i}$ and w_i (i = f or s) for both modes were determined. Herein, the term *apparent* means that the parameters were measured at certain scattering vector q and solution concentration c. The absolute values of the hydrodynamic radius, $R_{h,f}$ and $R_{h,s}$, and concentrations, c_f and c_s, of the scatterers were obtained by extrapolating these values to $q^2 \to 0$ and $c \to 0$.

The relative contributions of the scatterers of both types, A_f and A_s, into the total intensity of scattered light were estimated from the original, intensity weighted size distributions (Fig. 1a). After this, the absolute intensities of the scattered light, I_f and I_s, were calculated using Eq. (7). As soon as the concentrations c_f and c_s and the absolute excess scattering

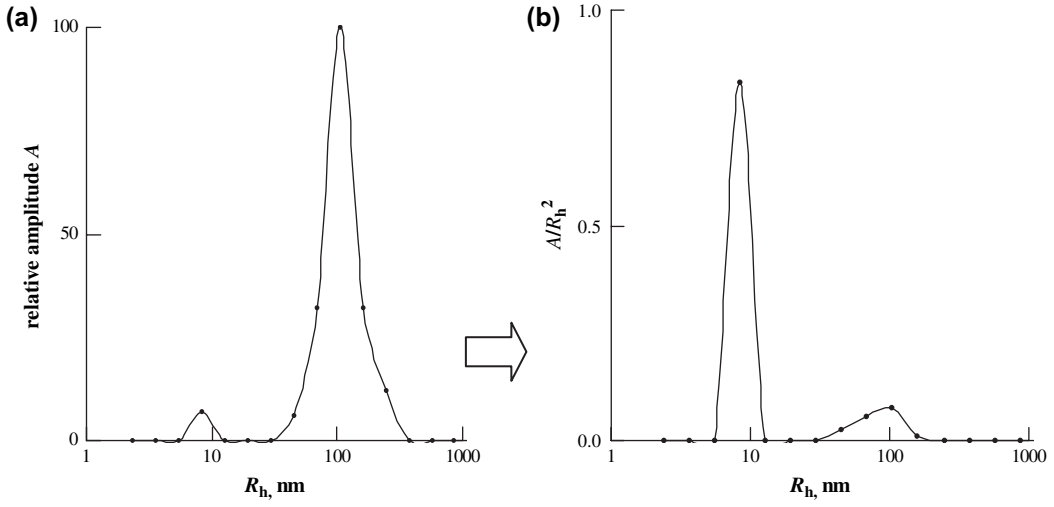

Fig. 1. Calculation of the mass weighted size distribution (b) from the intensity weighted size distribution (a) obtained at 90° scattering angle for sample 3 with the total concentration of 2.0 mg/ml.

intensities I_f and I_s of each mode are defined, it is possible to calculate the values of molar masses for each mode, $M_{w,f}$ and $M_{w,s}$, and the radius of gyration for the slow mode, $R_{g,s}$.

All the samples were analyzed with above described procedure and outlined in Eqs. (6)–(11). M_w, R_g, R_h and c were obtained and listed in Table 1. In this table the experimentally obtained weight-average values of M_w and R_g, R_h, calculated (before deconvolution) by standard techniques described in Section 2 are also present.

No angular dependencies of the absolute intensity of scattered light, I_f, and hydrodynamic radius $R_{h,f}$ was observed for the fast mode owing to the small, in respect to the wavelength, size of the scatterers. For that reason, the radius of gyration for the fast mode could not be estimated. The obtained molar masses, $M_{w,f}$, and $R_{h,f}$ are in a good agreement with those of the matrix PVP, see Table 1. However, the fast mode may also represent individual PVP/C_{70} complexes consisting of a single PVP molecule bound to a single (or to just a few) C_{70} molecule. To estimate the effect of a C_{70} molecule on the translation diffusion coefficient of the matrix PVP, the diffusion coefficient of C_{70} was estimated using Stokes–Einstein equation and assuming a hard sphere with a radius of 0.35 nm (for fullerene) [18]. The diffusion coefficient equals 0.6×10^{-7} cm^2/s and it is 1 order of magnitude lower than that of a single PVP molecule. Therefore, if there are fullerene molecules bound to the single PVP molecule, we can hardly detect them. At this stage, we can only conclude that the fast diffusive process most likely describes either the motion of a single PVP chain or that of a single chain, into which one or few fullerenes are bound.

In contrast to the fast mode, $R_{h,s}$ corresponding to the slow diffusion is a linear function of angle q^2. As $q \to 0$, $R_{h,s} = 50$–130 nm (see Table 1), which is significantly larger than R_h of the PVP. The fact that $R_{h,s}$ increases with decreasing q^2 suggests that the clusters are loose flexible structures. However, polydispersity of the clusters has to be considered as well.

In the above-presented procedure for estimation of the relative contributions of each of the scattering species into the total intensity (Eqs. (7) and (8)), the shape of the peaks was considered. Another modified procedure taking the shape of the peaks into account was applied for sample 5 as an example. In this case, the relative contributions were calculated as follows:

$$A_f = \frac{\sum_{\text{fast}} A_i R_{h,i}}{\sum_{\text{fast}} R_{h,i}}; \quad A_s = 1 - A_f \tag{12}$$

As is seen from Table 1, the molar mass and size of the scatterers of both types obtained by the modified procedure and marked in Table 1 with an asterisk sign, *, only slightly differ from the values calculated using Eqs. (6)–(11). However, the values of M_w for the fast mode obtained using Eqs. (6)–(11) are more close to the molar mass of the matrix PVP, M_{PVP}. For this reason all SLS and DLS data were further processed by Eqs. (6)–(11).

The weight-average molar mass, $M_{w,tot}^{calcul}$, consisting of f- and s-type scatterers was calculated and compared with the experimentally measured value, $M_{w,tot}$. By its definition $M_{w,tot}$ equals to the sum $M_{w,f}w_f + M_{w,s}w_s$, where $M_{w,f}$ and $M_{w,s}$ are the molar masses of particles and w_f, w_s are their relative weights. From the combination of the SLS and DLS data we estimated the values of w_f and $M_{w,f}$ for individual PVP and w_s and $M_{w,s}$ for clusters and $M_{w,tot}^{calcul}$ was calculated. The obtained values of $M_{w,tot}^{calcul}$ coincide with experimentally measured molar mass $M_{w,tot}$ within the experimental error of 10% for all the samples. It can serve as a checkpoint showing that the estimated molar masses and concentrations of the f- and s-type scatterers are correct.

The relative weights, w_f and w_s, provide information about the stability of the clusters against dilution. It is observed that the w_f and w_s do not depend on q^2, as expected. However, w_f and w_s also are independent of concentrations c, see Fig. 2. This fact points out that the clusters do not disintegrate upon dilution. Another evidence of stability of the clusters against dilution is that the hydrodynamic radius of the clusters, $R_{h,s}$, for all the samples studied is independent of concentration, see inset in Fig. 2. This finding is consistent with the results of the SLS experiments. Indeed, dissymmetry of the scattered light, z_θ, related to the size and shape of the particles remains invariable with decreasing the solution concentration. It means that the sizes of the clusters and their relative contributions into the total intensity of the scattered light do not change upon dilution.

The w_f and w_s averaged over all angles and concentrations are independent of M_{PVP} when fullerene content is kept constant. On the other hand, they show a slight dependence with changing the fullerene content in the complex, ϕ. As can be seen from Fig. 3, w_f somewhat decreases upon increasing the fullerene content whereas w_s increases. It may mean that an increase in ϕ causes a decrease in the number of free PVP molecules, not bound into the cluster. As a result the relative mass content of the clusters in solution increases.

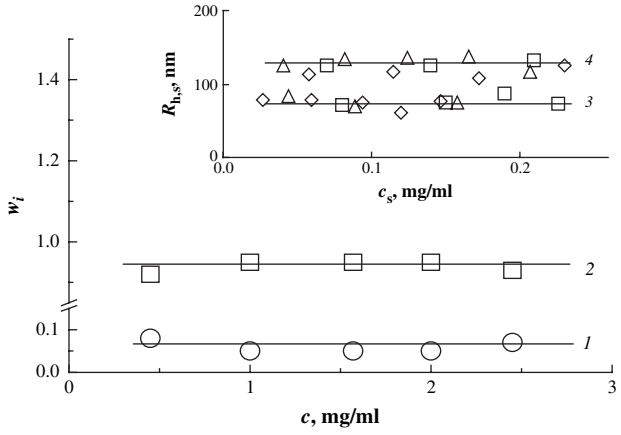

Fig. 2. Concentration dependences of the slow w_s (1) and of the fast w_f (2) modes for sample 4. Inset shows the concentration dependence of the hydrodynamic radius $R_{h,s}$ for the samples 1–7. Fullerene content in the complex is 0.4 wt% (3) and 0.6 wt% (4). Molar masses of the matrix PVP are 10×10^3 (triangle), 25×10^3 (diamond), and 40×10^3 (square) g/mol. Data obtained at 0° scattering angle.

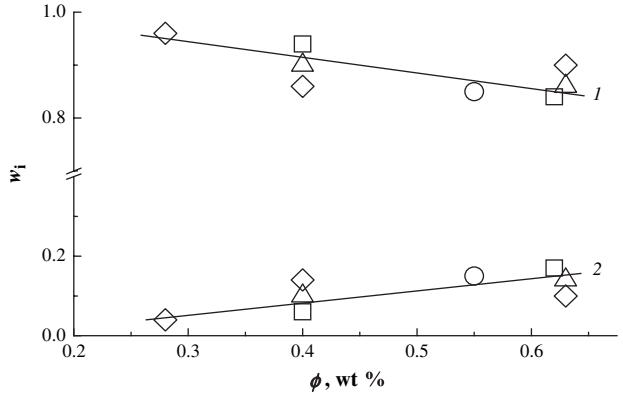

Fig. 3. The dependence of w_i (where i is either the fast (1) or the slow (2) mode) on the fullerene content ϕ in the complex formed by PVP of 10×10^3 (diamond), 25×10^3 (square), 40×10^3 (triangle), and 46×10^3 (circle) g/mol.

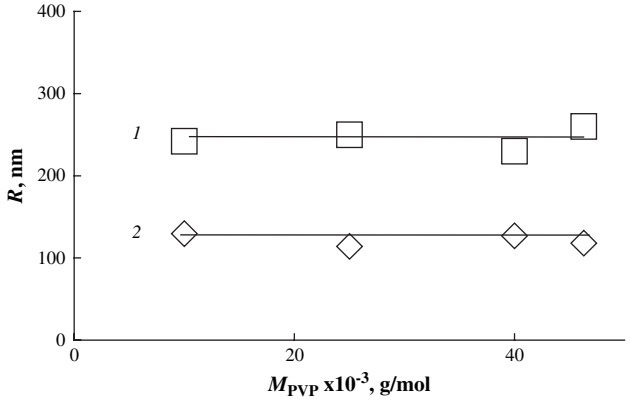

Fig. 5. The radius of gyration, $R_{g,s}$, (1) and the hydrodynamic radius, $R_{h,s}$, (2) plotted versus the molar mass of the matrix PVP, M_{PVP}, for the PVP/C_{70} clusters with $\phi \approx 0.6$ wt%.

It can also lead to an increase in size and the molar mass of the clusters. Indeed, the molar mass of the clusters $M_{w,s}$ and their size (both $R_{h,s}$ and $R_{g,s}$) increase with increasing the fullerene content ϕ as is seen from Fig. 4. In contrast, Fig. 5 reveals that an increase in M_{PVP} does not influence any parameters of the cluster, i.e. $M_{w,s}$, $R_{h,s}$ and $R_{g,s}$.

Now when the molar mass and size of the clusters have been estimated, the crossover concentration c^* of the clusters in solutions can be easily calculated via equation $c^* = 3M_w/(4\pi R_g^3 N_A)$ [17]. The obtained values for $c^* = 1.6$–2.3 mg/ml coincide with the values of critical concentrations $c_c = 1.8$–2.3 mg/ml, detected in SLS experiments. Thus, we can suppose that c^* is a crossover concentration of the clusters in solution. Our measurements were mainly done at concentration $c < c_c$ and thus below c^*. Single PVP molecules can actually decrease the crossover concentration c^*. However, linearity of all the concentration dependences studied below c_c suggests that this effect is minor.

Our calculations have been based on the assumption that the PVP/C_{70} clusters have a coil-like conformation ($x = 2$ in Eq. (9)). Now we will test the assumption. Firstly, the $M_{w,s}$ vs. $R_{g,s}^{\ x}$ plot passing through the center of coordinates is best fitted when $x = 2.2$ (not shown herein). This fact manifests the swollen, solvent-draining structure of PVP/C_{70} clusters; clusters have fractal dimension of $x = 2.2$, which represents slightly higher spatial packing of polymer material than for ideal coil with $x = 2$. This may seem to be in disagreement with the R_g/R_h ratio. However, the distribution of the repeating units within a cluster may differ from that within a coil. Thus density of a coil is the highest in the center of mass. More even density distribution within a solvent-draining structure may result in increasing R_g.

Secondly, Fig. 6 shows the dependence of R_h on M_w (in log–log scale) for PVP in water obtained using SLS and DLS and in aqueous 0.1 M sodium acetate obtained using diffusion–sedimentation analysis (data taken from Ref. [19]). The data for the PVP/C_{70} clusters in water are plotted on the same figure and fits the dependence M_w vs. R_h obtained for the PVP coil having similar molar masses as the clusters. It signifies that the clusters are not dense aggregates; otherwise the data for clusters would fall below the straight line.

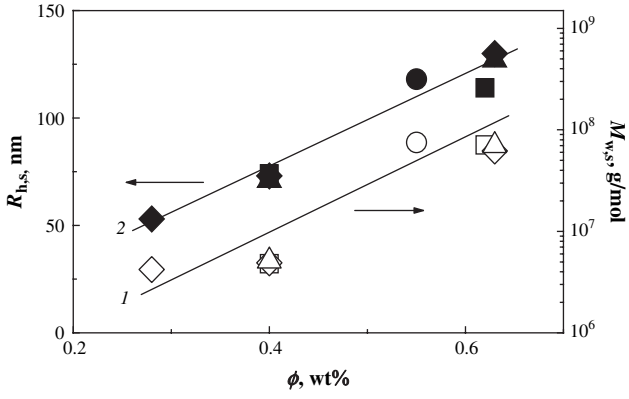

Fig. 4. The dependences of the molar mass $M_{w,s}$ (1; log-normal scale) and the hydrodynamic radius $R_{h,s}$ (2) of the PVP/C_{70} clusters on the fullerene content ϕ. The molar mass of the matrix PVP is 10×10^3 (diamond), 25×10^3 (square), 40×10^3 (triangle), and 46×10^3 (circle) g/mol.

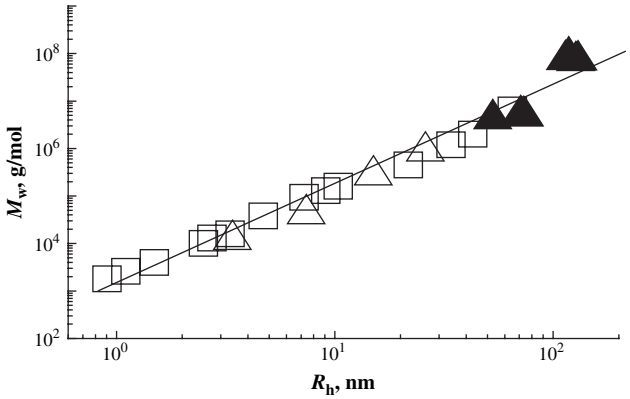

Fig. 6. The plots of M_w versus R_h for PVP. Squares: data taken from Ref. [19]; open triangles: matrix PVP studied herein; closed triangles: PVP/C_{70} clusters in water obtained from deconvolution of SLS and DLS data.

Thirdly, some information concerning the architecture of clusters can also be taken from the so-called Kratky plot [20]. In this plot the particle scattering factor $P(q) = I(\theta)/I(\theta = 0)$ is multiplied by $(qR_g)^2$ and plotted versus the parameter qR_g. Differences in architecture of particles become detectable only in the far q-region where $qR_g > 2$. The advantage of the Kratky presentation is that the asymptotic part at large qR_g is strongly amplified and this makes differences easily discernible. Fig. 7 shows the Kratky plot for several clusters. The scattering curves from the different clusters coincide with each other and with the theoretical curve obtained for coil-like macromolecules. As has been discussed in Ref. [21], the deviation of the experimental data from the theoretical curve at large q (their asymptotic increase) can originate from an excluded-volume interaction or/and from chain stiffness. Since water is one of the best solvents for flexible PVP chains, the excluded volume interaction is effective.

We tested the fractal dimension $x = 2.2$ of the clusters using Eq. (10) to estimate relative weights w_i (i = f or s) for sample 6 as an example. We found that in this case $M_{w,f}$, $R_{g,f}$, $R_{g,s}$ and w_f differ by 1–3% from the data obtained using $x = 2$. The value of $M_{w,s}$ decreased by 15%. Consequently, dependences shown in Figs. 1–6 were not affected.

From our data we reckon out the ratio of the number of the C_{70} molecules per number of PVP chains, N_{ful}/N_{PVP}, involved in a cluster. The ratio N_{ful}/N_{PVP} can provide insight into the internal organization of the cluster. After deconvolution of the total light scattering intensity, the concentration of clusters, c_s, was estimated and the average number of clusters in solution was calculated. Knowing the fullerene concentration we calculated the total number of fullerene molecules in solution. Assuming that all the fullerenes take part in formation of the clusters, we calculated the average number of fullerenes involved in a cluster, N_{ful}. The average number of PVP molecules in cluster, N_{PVP}, was calculated as $M_{w,s}/M_{PVP}$. Hence, the ratio of N_{ful}/N_{PVP} can be easily defined.

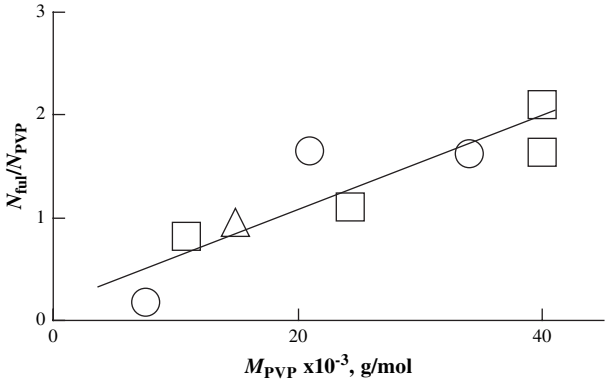

Fig. 8. The dependence of the N_{ful}/N_{PVP} ratio on the molar mass of the matrix PVP, M_{PVP}, obtained for the PVP/C_{70} clusters. The fullerene content is 0.28 (triangle), 0.4 (circle), and 0.6 (square) wt%.

Fig. 8 demonstrates the dependence of N_{ful}/N_{PVP} ratio on molar mass of PVP. As is seen, N_{ful}/N_{PVP} ratio increases linearly with increasing M_{PVP}. Such linear dependence suggests the existence of certain ratio of repeating units of PVP per C_{70} molecule. Fig. 9 shows the dependence of the (repeating units of PVP)/C_{70} ratio on M_{PVP}, which confirms our suggestion: there is a specific (PVP units)/C_{70} ratio ($\approx$200) which is same for all PVP/C_{70} complexes and independent of M_{PVP}, molar mass of clusters $M_{w,s}$, and fullerene content ϕ. One can also see from Table 1 that $M_{w,s}$ of the clusters with the same fullerene content $\phi = 0.62–0.63$ is the same. The fact that fullerene can bind only a certain number of PVP molecules has been also shown recently using the Kerr electro-optic effect in Ref. [22]. Owing to the existence of specific (PVP units)/C_{70} ratio it becomes evident why any cluster parameters do not depend on M_{PVP}. An increasing number of fullerenes binds more PVP molecules into a cluster with respect to this

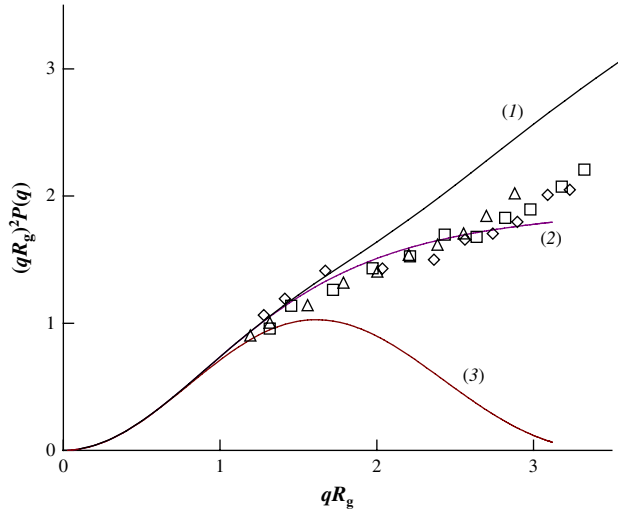

Fig. 7. Kratky plot $(qR_g)^2P(q)$ vs. qR_g of the experimental scattering function from clusters. The fullerene content in the complex $\phi \approx 0.4$ wt%. The molar mass of the matrix PVP is 10×10^3 (diamond), 25×10^3 (square), 40×10^3 (triangle) g/mol. For comparison, the theoretical curves for rods (1), coils (2) and hard spheres (3) are added.

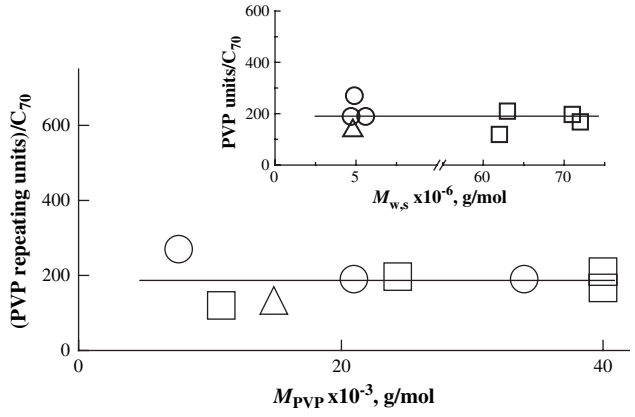

Fig. 9. The dependence of the (PVP repeating units)/C70 ratio on the molar mass of the matrix PVP, M_{PVP}, for the PVP/C70 clusters. Inset demonstrates the dependence of the (PVP units)/C70 ratio on the molar masses of the clusters, $M_{w,s}$. The fullerene content in the clusters is 0.28 (triangle), 0.4 (circle), and 0.6 (square) wt%.

ratio. Along with it, the cluster size increases with the fullerene content.

This ratio, perhaps, may be not a universal parameter, a constant for all types of polymer–fullerene complexes. It may depend on the chemical structure of used matrix polymer, the way of preparation of complexes, or the fullerene type.

4. Conclusions

Using a combination of DLS and SLS we deconvoluted the total intensity of light scattered by the aqueous solutions of the PVP/C_{70} complexes and thus found the true conformation of large PVP/C_{70} clusters. The value of $M_{w,s}$ for the clusters is higher than those for matrix polymer PVP by 1–2 orders of magnitude.

Clusters have large dimensions ($\sim$100 nm in average) that do not allow a star-like conformation with a fullerene core. It is more probable that the PVP/C_{70} cluster has a loose network-like structure where fullerenes serve as junction points for two or more PVP molecules. The $R_{g,s}/R_{h,s}$ ratio for clusters is 1.8 in average, which is typical for swollen, solvent-draining structures.

The PVP/C_{70} clusters are stable and do not disintegrate upon dilution. For all the samples studied no concentration dependence of the hydrodynamic radiuses $R_{h,s}$ was observed. Along with it, the mass fractions of the scatterers, w_i (i = fast or slow), and dissymmetry of the scattered light intensity are independent of the solution concentration showing that the ratio of single PVP molecules and clusters in solution is constant.

The size and the molar mass of the clusters increase upon increasing the fullerene content ϕ in the complex. However, if the fullerene content is kept constant, any of the parameters of the cluster are not affected by increasing the molar mass of matrix PVP.

Obtained results reveal the existence of a certain ratio of polymer repeating units per fullerene molecules (PVP units/C_{70}). This ratio ($\approx$200) does not depend on either the molar mass of the matrix PVP or the fullerene content. Probably, this ratio cannot be exceeded otherwise free fullerene molecules appear, which are not bound to PVP; PVP chains become saturated with fullerene and the fullerene molecules are no longer soluble in water. With lower fullerene concentration, free PVP molecules may exist in solutions.

Acknowledgements

Elvira Tarassova acknowledges the Laboratory of Polymer Chemistry, University of Helsinki for possibility to conduct the measurements. This work has been supported by the Center of International Mobility CIMO, Finland and by the Department of Chemistry and Material Science of the Russian Academy of Sciences, PFBR no. 05-03-33152.

References

[1] Da Ros T, Prato M. Chem Commun 1999;663.
[2] Friedman SH, Ganapathi PS, Rubin Y, Kenyon GL. J Med Chem 1998;41:2424.
[3] Rio Ya, Nierengarten J-F. Tetrahedron Lett 2002;43:4321.
[4] Lebedev VT, Torok G, Cser L, Len A, Orlova DN, Zgonnik VN, et al. J Appl Crystallogr 2003;36:646.
[5] Khairullin II, Yu-H Chen, Hwang L-P. Chem Phys Lett 1997;275:1.
[6] Andrievsky GV, Kosevich MV, Vovk OM, Shelkovsky VS, Vashchenko LA. J Chem Soc Chem Commun 1995;1281;
Gharbi N, Pressac M, Hadchouel M, Szwarc H, Wilson SR, Moussa F. Nano Lett 2005;5:2578.
[7] Sushko ML, Tenhu H, Klenin SI. Polymer 2002;43:2769.
[8] Klenin SI, Sushko ML, Dumpis MA, Poznyakova LI, Piotrovskii LB. Tech Phys 2000;45:312.
[9] Sushko ML, Aseyev VO, Tenhu H, Klenin SI. Mol Mater 2000;13:339.
[10] Tarassova EV, Aseyev OV, Tenhu H, Klenin SI. Polymer 2003;44:4863.
[11] Klenin SI, Tarassova EV, Aseyev VO, Tenhu H, Baranovskaya IA, Trusov AA, et al. Polym Sci 2004;46:68.
[12] Yamakoshi YN, Yamagami T, Fukuhara K. J Chem Soc Chem Commun 1994;517.
[13] Kratochvil P. Classical light scattering from polymer solution. Amsterdam: Elsevier; 1987.
[14] Siegert AJF. MIT Radiation Laboratory Report no. 4652; 1943.
[15] Klucker RK, Munch JP, Schosseler F. Macromolecules 1997;30:3839.
[16] Raspaud E, Lairez D, Adam M. Macromolecules 1994;27:2956.
[17] Burchard W. Adv Polym Sci 1999;143:113.
[18] Eletskii AV, Smirnov BM. Uspekhi Fizicheskih Nauk 1995;165:977.
[19] Pavlov GM, Panarin EF, Korneeva EV, Kurochkin KV, Baikov VY, Ushakova VN. Vysokomol Soedin A 1990;32:1190.
[20] Kratky O, Porod G. J Colloid Sci 1949;4:65.
[21] Savin G, Burchard W. Macromolecules 2004;37:3005.
[22] Evlampieva NP, Lavrenko PN, Zaitseva II, Melenevskaya EYu, Biryulin YuF, Vinogradova LV, et al. Vysokomol Soedin A 2002; 44A:1564.